A&A 376, 175–187 (2001)
DOI: 10.1051/0004-6361:20010950
© ESO 2001

Astronomy & Astrophysics

δ Scuti stars in Praesepe*

I. The STACC 1998 campaign – the photometry

S. Frandsen[1], A. Pigulski[2], J. Nuspl[3], M. Breger[4], J. A. Belmonte[5], T. H. Dall[1], T. Arentoft[6], C. Sterken[6,**], T. Medupe[7], S. K. Gupta[8], F. J. G. Pinheiro[9], M. J. P. F. G. Monteiro[9], C. Barban[10], M. Chevreton[11], E. Michel[10], J. M. Benkő[3], Sz. Barcza[3], R. Szabó[3], Z. Kołaczkowski[2], G. Kopacki[2], and S. N. Udovichenko[12]

[1] Institute for Physics and Astronomy, University of Aarhus, Universitetsparken, Bygn. 520, 8000 Aarhus C, Denmark
[2] Institute of Astronomy, Wrocław University, Kopernika 11, 51-622 Wrocław, Poland
[3] Konkoly Observatory, 1525 Budapest XII, PO Box 67, Hungary
[4] Institut für Astronomie, Türkenschanzstrasse 17, 1180 Wien, Austria
[5] Instituto de Astrofísica de Canarias, 38200 La Laguna, Tenerife, Spain
[6] Astronomy Group, University of Brussels (VUB), Pleinlaan 2, 1050 Brussels, Belgium
[7] South African Astronomical Observatory, PO Box 9, Observatory 7935, Cape, South Africa
[8] UP State Observatory, Manora Peak, Nainital – 263 129, India
[9] Centro de Astrofísica da Universidade do Porto, rua das Estrelas, 4150-762 Porto, Portugal
[10] Observatoire de Paris, DASGAL, UMR 8633, 92195 Meudon, France***
[11] Observatoire de Paris, DAEC, UMR 8632, 92195 Meudon, France
[12] Odessa Astronomical Observatory, Park Shevchenko, Odessa 270014, Ukraine

Received 20 April 2001 / Accepted 27 June 2001

Abstract. We present the results of the multisite differential CCD photometry for the two δ Scuti stars, BN and BV Cnc, in the open cluster Praesepe. The main objective was to identify the character of the pulsation modes in BN Cnc deriving their accurate periods, amplitudes and phases. These parameters are essential for the mode identification which uses combined photometric and spectroscopic data and is presented in the second article. For BN Cnc, six pulsation modes with amplitudes above the detection limit (~0.5 mmag) were detected. Using the same CCD frames it was possible to verify the presence of the four pulsation modes in BV Cnc, the faintest of δ Scuti stars in Praesepe. It is shown that in this very low-amplitude pulsator, substantial amplitude variations are seen between 1997 and 1998.

Key words. stars: oscillations – stars: variable: δ Scuti – open clusters and associations: individual: Praesepe

1. Introduction

Current efforts to improve the understanding of stellar evolution include asteroseismology as the most promising technique. Several space programs are underway. COROT (Baglin et al. 2001) and MONS (Kjeldsen et al. 2000) mainly address observations of solar-like oscillations, whereas MOST (Matthews et al. 2001) will observe also pulsators with higher amplitudes. All projects have among their main targets one or more δ Scuti stars. The rich set of oscillation modes in these stars make them very attractive for seismic investigations.

Ground-based observations play a particularly important part in the studies of this group of stars. Even though δ Scuti stars with 20–30 modes are observed, the comparison and identification of these modes with model frequencies has proven to be very difficult. Two methods have been attempted in order to solve this:

1. Extensive observations of a carefully selected single star. This consists of several large multisite photometric campaigns, supplemented by time-series spectroscopy. The results presented at a recent workshop in Vienna show that only for one star, FG Vir (Breger et al. 1999), we do begin to close in on the right models.

Send offprint requests to: S. Frandsen, e-mail: srf@ifa.au.dk

* Based in part on observations obtained at the European Southern Observatory at La Silla, Chile (Application 60D-0148).

** Research Director, Fund for Scientific Research (FWO).

*** *Present address of C.B.*: National Solar Observatory, 950 N. Cherry Ave., Tucson, AZ 85719, USA.

Article published by EDP Sciences and available at http://www.aanda.org or http://dx.doi.org/10.1051/0004-6361:20010950

This is mainly due to a successful identification of a small set of modes in this star (Viskum et al. 1998). To be more precise, the situation might be even more exciting in the sense, that none of the models fit, but this still depends on an uncertain mode identification. For another star XX Pyx (Pamyatnykh et al. 1998) with a similar rich oscillation spectrum the comparison of observed and model frequencies still leaves a large set of models, which all could represent the star. This is due to the lack of information about the mode type of the oscillation with a given observed frequency. The star is faint and the only available spectroscopy (Handler et al. 1997) does not have good enough time resolution to be of use for mode typing;

2. The second method is to observe variables in clusters and then analyze them together. The additional constraints derived from the knowledge of the distance, age and composition of the cluster can be used to narrow down the parameter range, which needs to be surveyed. In this case the choice of variables is among a small set of stars, and one does not have as rich a set of oscillating modes as for the best field stars. This approach has been applied to the δ Scuti stars in the open cluster Praesepe, where a series of photometric campaigns have taken place (see below) and the Pleiades (Fox Machado et al. 2001). A quite clear dependence of the frequency content on luminosity for δ Scuti stars in Praesepe (Belmonte et al. 1997) indicates that the method can indeed be successful.

The current campaign of the STACC network (Frandsen 1992) is in a way an attempt to do both. This paper (Paper I) describes the photometric results from a large multisite campaign with data over a period from January to April 1998 on the two stars, BN Cnc and BV Cnc. The purpose of the photometry is to characterize the oscillation spectrum as well as possible and to determine accurate amplitudes for the main modes in BN Cnc. This is needed for Paper II (Dall et al. 2001), which will describe the spectroscopic results for BN Cnc obtained from other sites using larger telescopes. A preliminary analysis of the spectroscopic data was presented by Dall (2000). In Paper II the photometric and spectroscopic results are combined and the modes identified.

If a good model can be found for one star (BN Cnc) and accurate parameters determined, then all common parameters (distance, [Fe/H], age) can be transferred to the 13 other variables, putting strong constraints on possible models for these stars.

2. δ Scuti stars in Praesepe – status

Praesepe has a nice group of δ Scuti stars consisting of 14 members (Rodríguez et al. 2000). For eight of these stars (not including BV Cnc) models are discussed by Michel et al. (1999) and the frequencies and amplitudes are summarized by Belmonte et al. (1997) and Hernández et al. (1998b, 1998c). Out of all δ Scuti stars in Praesepe, nine have been the targets of multisite observations. BU and EP Cnc were observed by the DSN (Delta Scuti star Network) (Breger et al. 1993, 1994). The STEPHI team observed BU, BN Cnc and KW 284 (Belmonte et al. 1994) and later BQ and BW Cnc (Álvarez et al. 1998) and BS and BT Cnc (Hernández et al. 1998a). Finally, BN Cnc and BV Cnc were observed by Arentoft et al. (1998), but only from a single site. All the stars listed have been shown to be multimode pulsators.

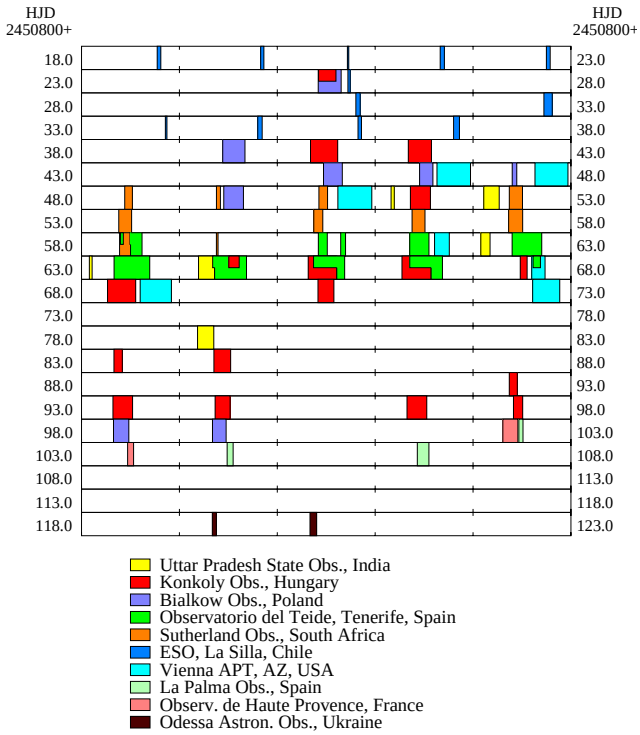

Fig. 1. Distribution of the photometric observations of BN Cnc carried out during the 1998 STACC campaign. Five consecutive nights are shown in each row.

3. The observations

The STACC 1998 campaign on BN and BV Cnc is the first large-scale photometric campaign based (mainly) on the differential CCD photometry aimed at δ Scuti stars. Using CCD cameras one can observe both stars simultaneously.

Ten sites participated in the photometric observations, which took place from January to April 1998. A variety of instrumentation was used and the number of nights allocated varying from a few nights to several weeks.

The number of useful nights was considerably lower than expected due to an unusual bad observing season at several sites. In Fig. 1 the nights with data are shown schematically for the participating sites (photometry only). In addition, spectroscopic data were obtained at five observatories. The main part of observing took place in February 1998. The distribution of sites did not provide a good 24-hour coverage. In Table 1 the instrumentation and observations are described in detail.

Table 1. Details on the observations and instrumentation.

Observatory	Telescope diam. [cm]	Detector	Filter(s) used	Field of view	Nights observed	Hours obtained	Remarks
Uttar Pradesh (India)	100	CCD	V	$6.6' \times 6.6'$	6	15.5	guiding problems
Konkoly (Hungary)	100	CCD	V	$5.3' \times 4.6'$	12	57.0	
	60	CCD	V	$27' \times 18'$	5	17.8	
Białków (Poland)	60	CCD	V	$6' \times 4'$	8	32.0	
Teide (Spain)	80	CCD	V	$7.3' \times 7.3'$	9	59.0	
Sutherland (S. Africa)	100	CCD	v, b, y, I_C	$3.4' \times 3.1'$	10	22.3	
ESO, La Silla (Chile)	90	CCD	y	$3.9' \times 3.9'$	12	11.5	
Vienna APT (AZ, USA)	75	PM	v, y	—	7	46.4	
La Palma (Spain)	100	CCD	V	$5.6' \times 5.6'$	3	7.2	
Haute Provence (France)	80	CCD	V	$6.4' \times 6.4'$	2	5.2	overexposed
Odessa (Ukraine)	50	CCD	V	$20' \times 20'$	2	2.6	high noise

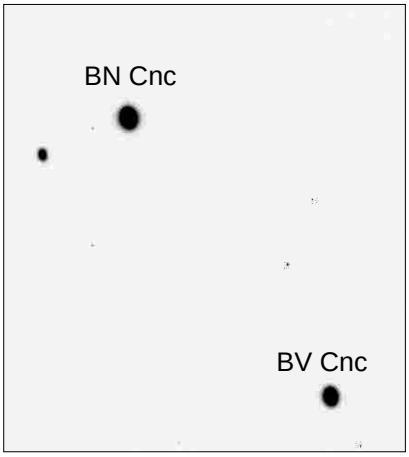

Fig. 2. A sample CCD frame of BN and BV Cnc field observed with the 1.0-m telescope at Sutherland Observatory. The two variables are labeled. North is up, east to the left.

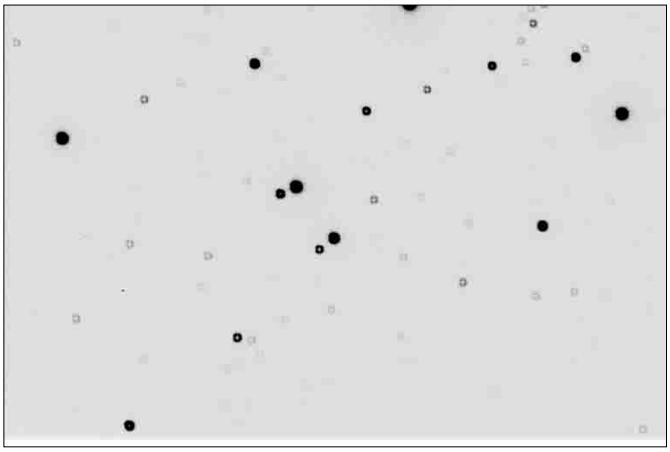

Fig. 3. A sample CCD frame observed with the 60-cm Schmidt telescope at Konkoly Observatory.

All sites except the Vienna APT in Arizona were using CCD cameras, but with quite a range in field of view and filters. A Johnson V filter was used at the majority of sites. At some sites (Sutherland, La Silla, Arizona) the observations were carried out in other filters (Strömgren vby, Cousins I_C). The differences in fields of view are best illustrated by displaying the two extreme cases. Figure 2 shows a CCD frame obtained at Sutherland, while Fig. 3 features a much larger field representing a frame from the 60-cm Schmidt telescope at Piszkéstető in Hungary. The latter clearly supplies a much larger set of reference stars for the two variable stars. The two variables both have close fainter stars, which in most cases are used as reference stars. These fainter stars are uncomfortably close, as a certain defocusing was needed to permit exposure times that give a decent duty cycle.

Some additional details on the observations at different sites are given here in separate paragraphs.

Uttar Pradesh State Observatory (UPSO). The data were obtained on 6 nights out of 20 allocated, which represent 15.5 hours of data. The longest set for one night covers 4.5 hours. Unfortunately, the frames do not carry a lot of weight in the total data set due to one failure in meeting the requirements for the campaign. The guiding failed to keep the two stars within a few pixels, and large flat-field effects are seen due to a drift of up to 30 pixels on a single night. This is particularly disappointing due to the few observatories joining the campaign at non-European longitudes.

Konkoly Observatory, Piszkéstető. Data from this observatory come from the 1.0-m RCC telescope, where around 6 weeks of observing time was allocated, and from the 0.6-m Schmidt telescope, where a smaller allocation was obtained late in the campaign. In terms of the climate this is not an outstanding site, but data were collected on 12 nights with the 1.0-m telescope and 5 nights with the 0.6-m telescope.

The large field of view and the corresponding larger set of bright comparison stars obtained with the Schmidt telescope has the effect that better results are obtained with the 0.6-m than with the 1.0-m telescope (see later in Table 4). For the data coming from all other telescopes in the campaign equipped with CCD, stars fainter than the

target stars BN and BV Cnc had to be used as comparisons.

Białków Observatory. The data were obtained on 8 nights. The results are of good quality and comparable to results obtained with larger telescopes proving that even a small telescope can make a significant contribution.

Observatorio del Teide. Thirteen nights were allocated and data collected on 9 nights. The lost nights were all at the beginning of the observing run. The data are of good quality, but effects of bad seeing and drifting clouds on some nights are traceable in the time series deduced from the CCD frames.

Sutherland Observatory. This site has one of the largest telescopes used in this campaign (1 m), but the field of view of its CCD camera is the smallest among all sites (Fig. 2). In consequence, only one comparison star could be used for these observations. Two weeks of time were granted and data collected on 10 nights. This illustrates a good climate at Sutherland, which is considered among the best photometric sites.

Observations were carried out in three Strömgren filters v, b, y plus the Cousins $I_{\rm C}$ filter.

The best signal-to-noise (S/N) was obtained in the v and b bands, where a larger amplitude more than compensates for the smaller number of photons. This is so much more true, because systematic effects dominate the noise budget making it almost colour independent.

European Southern Observatory (ESO). The 0.9-m Dutch telescope with a 1k $\times$ 1k CCD was used. Time was available a few hours on selected nights during another observing program, and data were collected early in the campaign on 12 nights. The longest set is only 2 hours long.

Weather conditions were variable and the quality varies quite a lot from night to night. Observing took place at large air masses and the telescope did not produce nice ringformed images when defocused, making the photometry difficult.

Vienna APT, Arizona. The observations were carried out with one of the two 0.75-m automatic photoelectric telescopes (Vienna APT's) located at Washington Camp in Arizona, USA. The data aquisition was performed with a blue-sensitive bi-alkali EMI-9124/QB photomultiplier and Strömgren v and y filters. The water-cooled tube is operated at a temperature of 3 °C and has a typical dark current of 20 counts s^{-1}. A detailed description of the APTs and the attached equipment can be found in the paper by Strassmeier et al. (1997).

The telescopes have been used before in the campaigns on other δ Scuti stars with the three-star technique of alternating observations of the variable star and two comparison stars. This technique allows for a check of the accuracy of the measurements. For the star 4 CVn, Breger & Hiesberger (1999) found a precision of 3.0 mmag in y for all three stars. For a 9th magnitude star, BI CMi, the precision decreases to 3.8 mmag per single observation under good weather conditions.

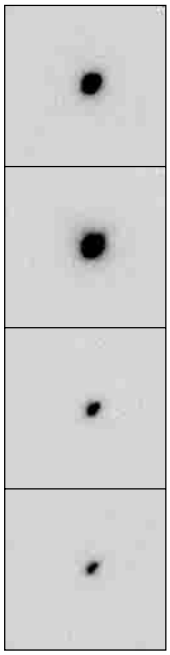

Fig. 4. An example of an OHP image of the program stars. The stars are repositioned one above the other with the two target stars at the top and two reference stars at the bottom.

The whole month of February was allocated, but due to the poor weather the data were taken on only 7 nights and only for a substantial part of the night on 5 nights. This is much below normal.

As this is one of a few sites off European longitudes this is again disappointing and to some extent makes the multisite character of the campaign less useful.

The quality of the data varies dramatically with weather conditions and is overall somewhat more noisy than the CCD photometry.

Observatorio del Roque de las Muchachos. Time was allocated fairly late in the campaign on the JKT telescope at La Palma. Six partial nights (3 hours each) were at disposal, and useful data were obtained on half of them.

Observatoire de Haute Provence (OHP). At OHP some test observations were spent on two nights observing BN and BV Cnc with a CCD camera using a new CCD controller. The controller is more advanced than the usual CCD controllers and permits to read out only windows around selected stars, which are then reorganized in a vertical stack. One example is shown in Fig. 4.

Unfortunately, due to the trial nature of the observations, the variable stars were slightly overexposed and although some decorrelation was attempted, it did not

bring the noise down to levels, where the data contribute significantly to the final result.

The windowing technique is interesting, because the duty cycle is higher than for other sites, and there is no reason to believe the results had been less good than from full frame observations had the overexposure not happened.

Odessa Astronomical Observatory. Another couple of nights were added from the Ukrainian site. The data are of lower quality than those from the sites providing the main part of the data.

3.1. Summary of observations

Only at a few sites was the number of clear nights a large fraction of the allocated time. This is often the case for northern observatories, especially in winter, except for the permanently good sites like the Canarian Islands or Hawaii. The Vienna APT site was considerably below normal owing to bad weather conditions caused by the El Niño.

It would clearly make this type of campaigns much more manageable, if telescopes and CCD cameras could be remotely operated in automatic or semi-automatic mode. In addition, telescopes should be situated at sites with a good photometric climate.

4. Photometric reduction

Most teams delivered completely reduced photometric time series for the two stars. Thus, several photometric reduction packages have been used. The choice has been made by the observing teams. In a couple of cases the raw data were transmitted and reduced by the PI.

The frames from Tenerife, ESO, OHP and UPSO were reduced using the differential photometry package MOMF (Kjeldsen & Frandsen 1992). The OHP frames were delivered as calibrated frames. The UPSO frames did not include an overscan strip. Bias frames had to be subtracted interpolating to the nearest in time. Due to the heavily defocused images, numerical binning had to be applied to some of the data to have the stellar diameters fitting the normal size of the Point Spread Function (PSF) in the MOMF package.

In addition to the magnitudes as a function of time, information about the image translation, the sky background and the seeing was recorded. Correlations with these household parameters or other parameters were checked and decorrelation attempted if dependencies were seen. This was absolutely needed for the OHP and UPSO data due to the problems described in the previous section.

The data from Vienna APT arrived as tables of magnitudes as a function of time for three stars: the two variable stars and a reference star. To reduce the effect of photon noise from the reference star on the differential magnitudes, a low-order smooth fit was made to the flux of the reference star, and this fit was then interpolated in time and subtracted from the two variable stars.

The Konkoly data were reduced by the method described by Arentoft et al. (1998) using a library of yet unpublished C functions.

The images from La Palma were reduced using DAOPHOT and the IRAF image reduction tools. DAOPHOT was also used for the reduction of the data from Białków.

The CCD frames obtained at Sutherland were reduced using DoPhot, and finally no information is available on the reduction techniques employed at the Odessa site.

The reduced data represent differential magnitudes (with respect to one or more comparison stars, depending on the site) with a mean difference subtracted.

5. Data merging and weighting

The light curves from the different sites and nights constitute a rather inhomogeneous sample. Combining these data is far from trivial. In order to see how some subjective decisions which must be made at this stage affect the final result, the merging and time-series analysis has been carried out independently by two teams and the results compared. It should be noted that the zero point corrections and detrending we apply for our data at the merging state suppress all low-frequency ($\sim$2 d^{-1} and smaller) signals, both spurious and real, if such are present.

5.1. Aarhus, method 1

Merging the data we try to correct for zero point offsets due to e.g. variable extinction and to adjust the scale in order to match different instrumental systems used at different sites.

The merging was done as an iterative process, where a number of free parameters were introduced and then fixed, either because a good value could be determined or a default value had to be chosen. Sometimes the datasets were too small or too noisy to allow for any but the simplest choice of parameters.

In the first step, the data made in b and v bands were transfered to a common scale with V-filter using scaling ratios of $b/y \sim 1.24$ and $v/y \sim 1.44$ derived from Viskum et al. (1998) observations of FG Vir. Because of the large scatter, the $I_{\rm C}$-filter observations were not used. The y and V amplitudes were assumed to be identical. The data were next divided into separate sets consisting of one-night observations from each site.

The parameters employed in the merging were then for each set: a correction for the zero point of the magnitude scale, a scaling factor (close to 1 and identical for all datasets with the same filter from one site) and a *subjective* quality factor, which was used to adjust weights applied in the time-series analysis.

Starting off with zero-point correction equal to zero, scaling factors of 1 and identical quality factors, a first

fit of a light curve to the data was derived. Subtracting the current fit from the data points, zero points and scaling values were derived and used to replace the original parameters. Also, a weight for each data point was calculated based on a smoothed value of the rms deviation at each time. This weight was multiplied by the quality factor. Sigma clipping was also applied by giving zero weight to outliers.

The zero point offsets found were small and the scaling factors in most cases not significantly different from 1.0. The scaling from v and b to V with factors 1.24 and 1.44 was however slightly modified. A certain amount of subjective decisions entered into this process: when to stop iterations and freeze the parameter set.

Because the main effort has been to reduce the noise by improving the weights, several principles were used to derive weights:

- The subjective approach: the first set of applied weights was a combination of weights calculated from a sliding mean of rms deviations of the data from the current synthetic lightcurve combined with weights derived from the photon counts. Also the subjective quality factors mentioned above entered here. These weights were calculated before merging the data;
- The objective approach: weights based on rms deviations, but filtered with a Gaussian function in time with a selected bandwidth. These weights were calculated for the combined dataset;
- Additional weighting scheme has been implemented in the Period98 code used for analysis (see Sect. 6.1), which generates weights according to the deviation of each point from a given fit. Weights are constant up to a given deviation, say 2σ, and then decrease as the deviation increases. We assumed that we have 2σ equal to 8 mmag. Thus, all points with deviations less than 8 mmag get weights 1.0, but a 10 mmag deviation gets a weight of $(8/10)^2$. The threshold should not be chosen too low and one should not iterate too many times as the solution then becomes unreliable.

All the above weights were applied and results compared throughout the analysis 1 described in the next section.

5.2. Wrocław, method 2

Because in method 1 scaling factors were found to be close to 1 for V and y observations, in the second approach no scaling of light curves made through different filters was performed. Since most of the data were obtained in Johnson V and Strömgren y bands, only these data were included. Because of different quality and sampling times, the emphasis was laid on a proper weighting of data. Low-quality nights were rejected from the analysis. Moreover, some data sets were freed from the instrumental low-frequency variations. This was done by fitting a sinusoid with a dominant frequency and allowing a linear time-dependent trend which was later subtracted.

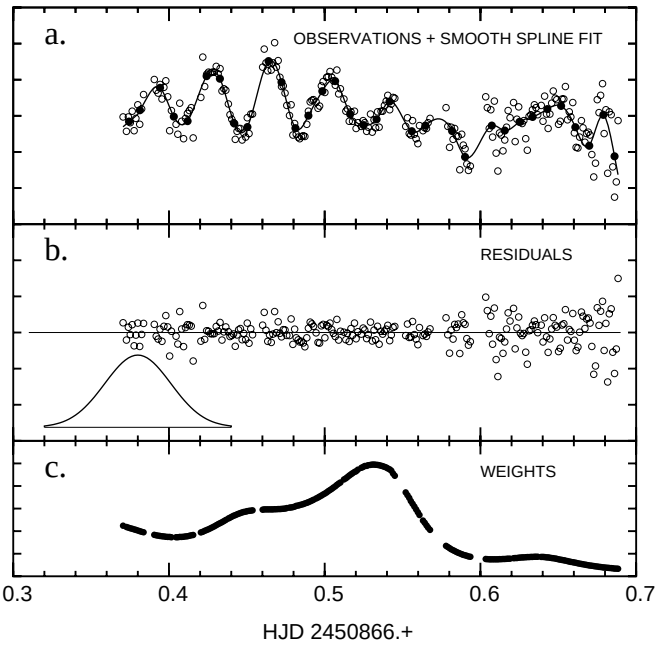

Fig. 5. An example of the calculation of weights in method 2: Observatorio del Teide observations carried out on 1998 February 21/22. **a)** Observations (open circles), 0.008-day averages (filled circles), and smooth spline fit (continuous line). **b)** Residuals from the fit shown in panel **a)**. For comparison, the weighting function (truncated Gaussian) is shown in scale. **c)** The weights (in arbitrary units).

An example of the calculation of weights within method 2 is shown in Fig. 5. The weights were assigned to each point individually. As we wanted the weights to be inversely proportional to the local variance, the procedure of calculating weigths was the following. Firstly, the real light variations were fitted by calculating averages in 0.008-day intervals and smoothing them by a spline fit (Fig. 5a). The resulting residuals (Fig. 5b) were next used to derive the local variance. This variance was calculated in a common way, but additional weighting of residuals was introduced in order to secure that only the points closest to a given one contribute to the local variance. This weighting function, a truncated Gaussian with $\sigma = 0.03$ d, is also shown in Fig. 5b. Finally, weights were calculated, as the inverse of the local variance multiplied by an arbitrary scaling factor. As can be seen in Fig. 5c, the weights indeed change accordingly with the changing scatter in residuals. We also point out that this procedure includes no assumption on the frequency content of the real signal.

6. Time-series analysis

As noted in the previous section, two independent time-series studies of the BN and BV Cnc photometry have been carried out. The objective is to find the best solution of the type

$$f(t) = \sum_{i=1}^{n} A_i \sin(2\pi\nu_i t + \phi_i), \quad (1)$$

which defines the amplitudes A_i, the frequencies ν_i and the phases ϕ_i.

6.1. Analysis 1

After cleaning the data with method 1, of the order of 7200 data points remained for BN Cnc and around 6800 for BV Cnc. To this we added about 620 points for BN Cnc and 680 for BV Cnc from 1997 obtained by Arentoft et al. (1998). The data from both seasons were combined together at the final stage of our analysis.

Periods, amplitudes and phases for a set of modes have been derived using the code Period98 (Sperl 1998) in its standard version and also in a version with a different weigthing scheme (see Sect. 5.1). In principle, Period98 uses Fourier periodogram and non-linear least-squares within its prewhitening process. In addition, the results from Period98 have been checked and special weighting procedures applied earlier by Frandsen et al. (1996) have been used.

6.2. Analysis 2

The data merged and weighted in a way described in Sect. 5.2 were used in analysis 2. Because in this approach some observations from the campaign were not used, the 1998 input dataset consisted of about 5000 data points for BN Cnc and rougly 4500 for BV Cnc. For 1997, the numbers were approximately the same as in analysis 1. In analysis 2, the least-squares (LS) periodogram allowing different weights was applied. In principle, the $p(f) = 1 - V_{\rm post}/V_{\rm pre}$ parameter plotted against the sample frequency f was used as a periodogram. The $V_{\rm pre}$ and $V_{\rm post}$ are the variances calculated prior to ($V_{\rm pre}$) and after ($V_{\rm post}$) fitting a sinusoid with a given frequency f to the data. In addition, the amplitude of a fitted sinusoid with frequency f was plotted as a second periodogram (hereafter, this will be called the LS amplitude periodogram). A detection of consecutive frequencies was done, like in analysis 1, by prewhitening with all previously found frequencies.

6.3. Comparison

The consecutive steps of the prewhitening with both kinds of time-series analysis are shown in Figs. 7 and 8 for BN Cnc and BV Cnc 1998 data, respectively.

The final results seem to be fairly robust in terms of a good agreement between the sets of oscillating modes for each variable derived using different weights and different programs. Although there are 1 d^{-1} differences in case of BV Cnc, the frequencies are derived in the same sequence by both methods. There are, however, small differences which need to be commented.

For BN Cnc (Fig. 7) the two methods yield, within the errors, the same frequencies F1 to F5. Although in analysis 2 the alias peak at F1$-$1 d^{-1} is higher than F1, the analysis of the combined 1997 and 1998 data (as well as the results from the STEPHI campaign, which had a better spectral window, Belmonte et al. 1994) leaves no doubt that the true frequency is F1 $\approx$ 25.76 d^{-1}, found as highest by analysis 1. Consequently, a sinusoid with frequency F1 was subtracted in the first step of prewhitening in analysis 2 as well. The largest difference ($\Delta \approx$ 0.044 d^{-1}) was obtained for the last frequency we derive, that is, F6. Again, combined 1997 and 1998 data indicate that F6 = 25.4351 d^{-1} is the correct one. We note that these different F6 frequencies are $1/\Delta \approx$ 23-day aliases, and 23 d is the average time difference between our 1998 January/February, late February and March groups of data (see Fig. 1). The amplitudes found in analysis 1 and 2 agree within the 3σ error, although, on average, analysis 2 gives them higher by 0.13 mmag.

For BV Cnc (Fig. 8) the situation is more confusing. As can be seen in Fig. 8, there is a strong aliasing problem for all three frequencies we find in the 1998 data. Like for BN Cnc, analysis 2 gives slightly higher amplitudes.

Because the results of analysis 1 and 2 are quite consistent (within the errors), we decided to present in a tabular form only the results of analysis 1. The differences we indicated above give an evaluation of the systematic errors which can be introduced at the subjective stage of merging and weighting the data of different quality.

To illustrate the data, selected nights are displayed in Fig. 6 together with the best fit found. On some dates data come from two sites.

7. What's new?

The result of our analysis is an unambiguous determination of a small set of frequencies in BN and BV Cnc, and a low upper limit on the amplitudes of possible additional modes. We now comment in detail the frequency spectra of both stars and compare them with previous studies.

7.1. BN Cnc

For this star we detect six modes. Five of them were known before and only one additional mode (F6) is new in comparison to earlier measurements (Belmonte et al. 1994; Arentoft et al. 1998). With the new dataset any alias problems have disappeared. Even though the sidelobes are still there, the S/N (see Table 2) is so good that there is no room for ambiguity. The frequency resolution is so high that it is improbable that any unresolved modes will be found.

Table 2 lists the modes we have detected with references to the analysis of Arentoft et al. (1998) indicated. Within the uncertainities, the amplitudes of the five dominant modes (except maybe F1) seem to be constant from 1997 to 1998. Two modes (F4 and F5) were weaker during the STEPHI campaign in 1992 and have increased amplitudes by roughly a factor of two. STEPHI had one more significant mode (A3) which, however, is different from the F6 mode. Two additional frequencies (A6 and A7) are

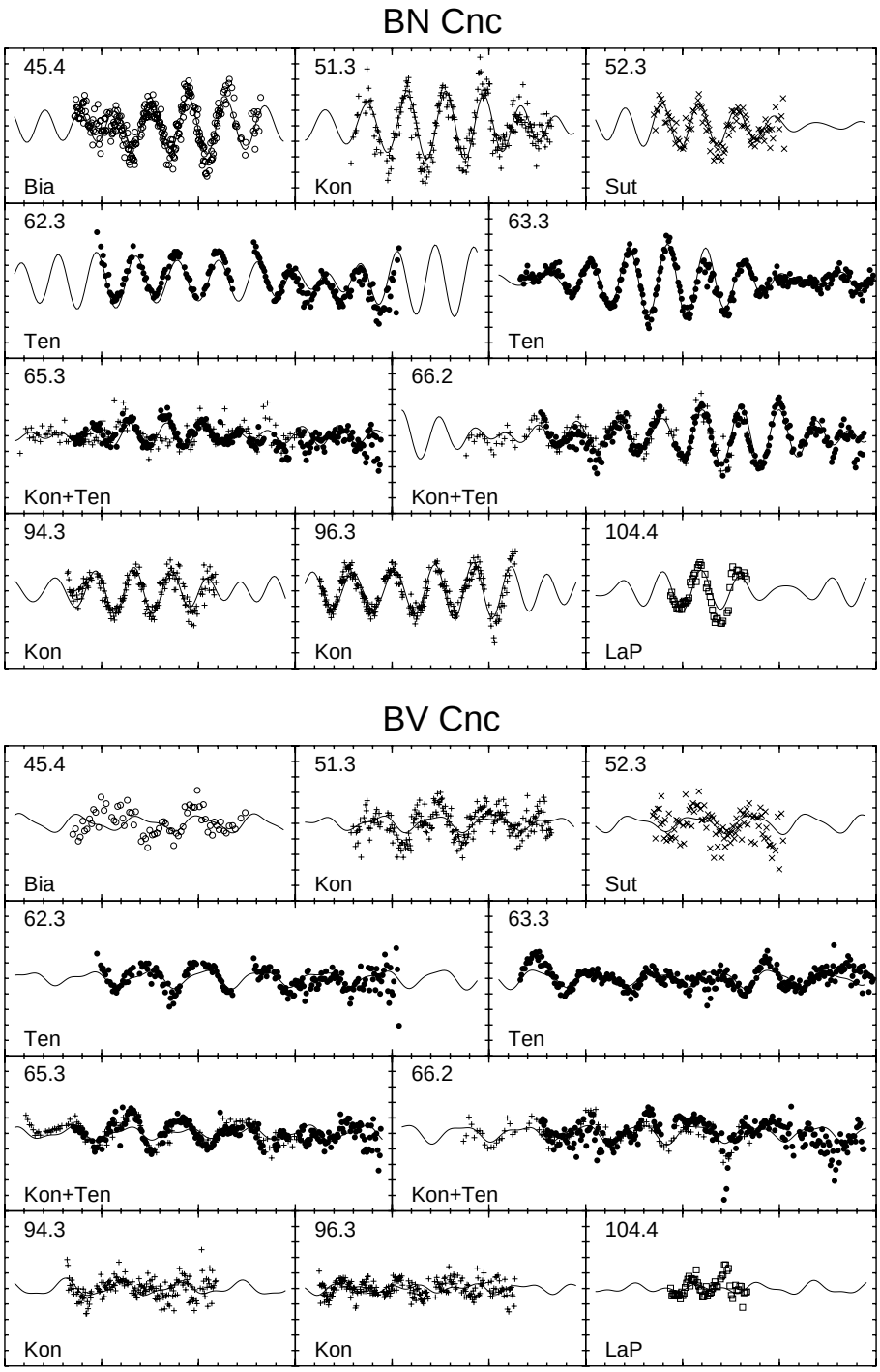

Fig. 6. Selected nights of the 1998 photometry of BN and BV Cnc. The data were prepared according to method 1, the solid line corresponds to the fit taken from analysis 1 and given in Tables 2 and 3 for BN and BV Cnc, respectively. The number in each panel presents the HJD with 2 450 800 subtracted for the origin of the X-axis. Short tick marks are spaced 0.02 d. The tick marks on the Y-axis are separated by 5 mmag. The second label indicates the site(s) from which the data come: Bia – Białków, open circles, Kon – Konkoly, plus signs, Sut – Sutherland, crosses, Ten – Tenerife, dots, and LaP – La Palma, squares.

listed by Arentoft et al. (1998), both with $S/N < 3.0$ in 1997 data, and none of them was recovered in the present larger dataset.

The noise level we obtained is around 0.12 mmag on the short side of the oscillation frequencies in the interval 8–15 d^{-1} and decreases to a white noise level of 0.07 mmag around 45 d^{-1}. Modes with amplitudes above 0.5 mmag should be therefore detectable. For the rereduction of the STEPHI data, the corresponding noise levels were 0.17 mmag and 0.11 mmag (Arentoft et al. 1998). After removal of six modes, the residuals show only a small excess just below 30 d^{-1}, indicating either some non-detected modes or perhaps inadequate removal of the signal. If there were indeed more modes with amplitudes

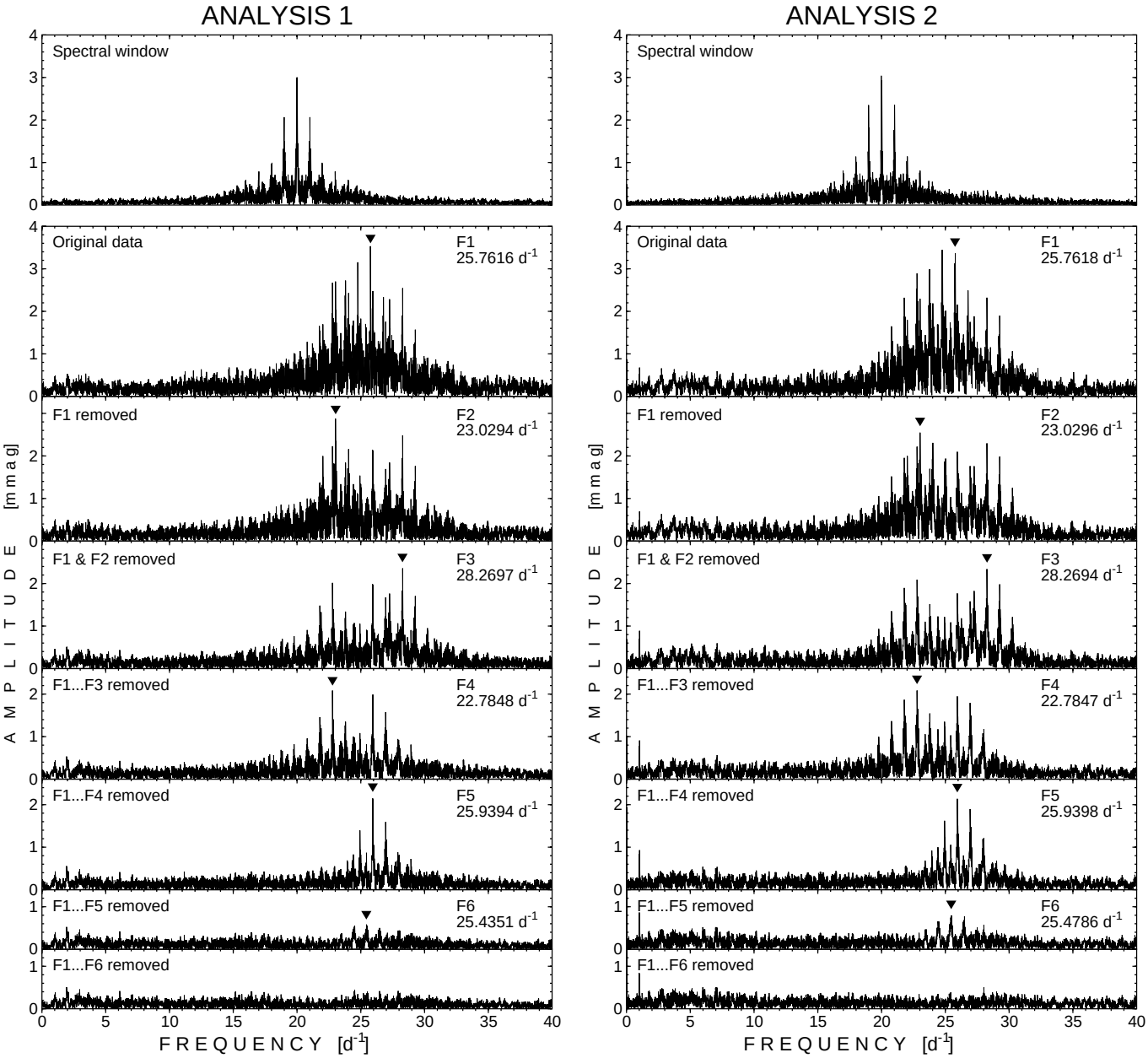

Fig. 7. Frequencies detected in the 1998 photometry of BN Cnc. The triangles indicate which frequencies were subtracted in the consecutive steps. Left: prewhitening process within analysis 1. These are Fourier periodograms. The spectral window is shown at the top panel. Right: the consecutive steps of prewhitening within analysis 2. The periodograms are the LS amplitude periodograms. The high peak at frequency 1 d^{-1} is an artifact produced by the method.

Table 2. Modes detected in BN Cnc. The frequencies, phases, and S/N values refer to the combined 1997 and 1998 data. The 1992 amplitudes come from the Arentoft's et al. (1998) reanalysis of the STEPHI 1992 observations (Belmonte et al. 1994). The frequencies labeled as $\nu(97)$ and former ID were taken from Table 4 of Arentoft et al. (1998). Errors are given in parentheses for the last digits.

Our	Former	Frequency		Amplitudes [mmag]				Phase		$\nu(97)$
ID	ID	[d^{-1}]	[μHz]	1992	1997	1998	1997+1998	[rad]	S/N	[μHz]
F1	A4	25.76114(04)	298.1614(05)	2.0	2.00(27)	3.01(8)	2.92(7)	4.87(03)	26	298.01
F2	A2	23.02981(05)	266.5487(05)	2.1	2.08(26)	2.52(8)	2.48(7)	1.70(03)	20	266.42
F3	A8	28.27039(05)	327.2036(05)	2.7	1.99(23)	2.42(8)	2.38(7)	3.08(03)	23	327.16
F4	A1	22.78352(05)	263.6981(06)	1.2	1.80(27)	2.32(8)	2.29(7)	5.08(03)	17	263.69
F5	A5	25.93964(05)	300.2273(06)	0.9	2.33(25)	2.13(8)	2.13(7)	3.87(03)	24	300.24
F6	–	25.43666(17)	294.4057(19)	—	0.92(24)	0.63(8)	0.67(7)	1.88(11)	6	—

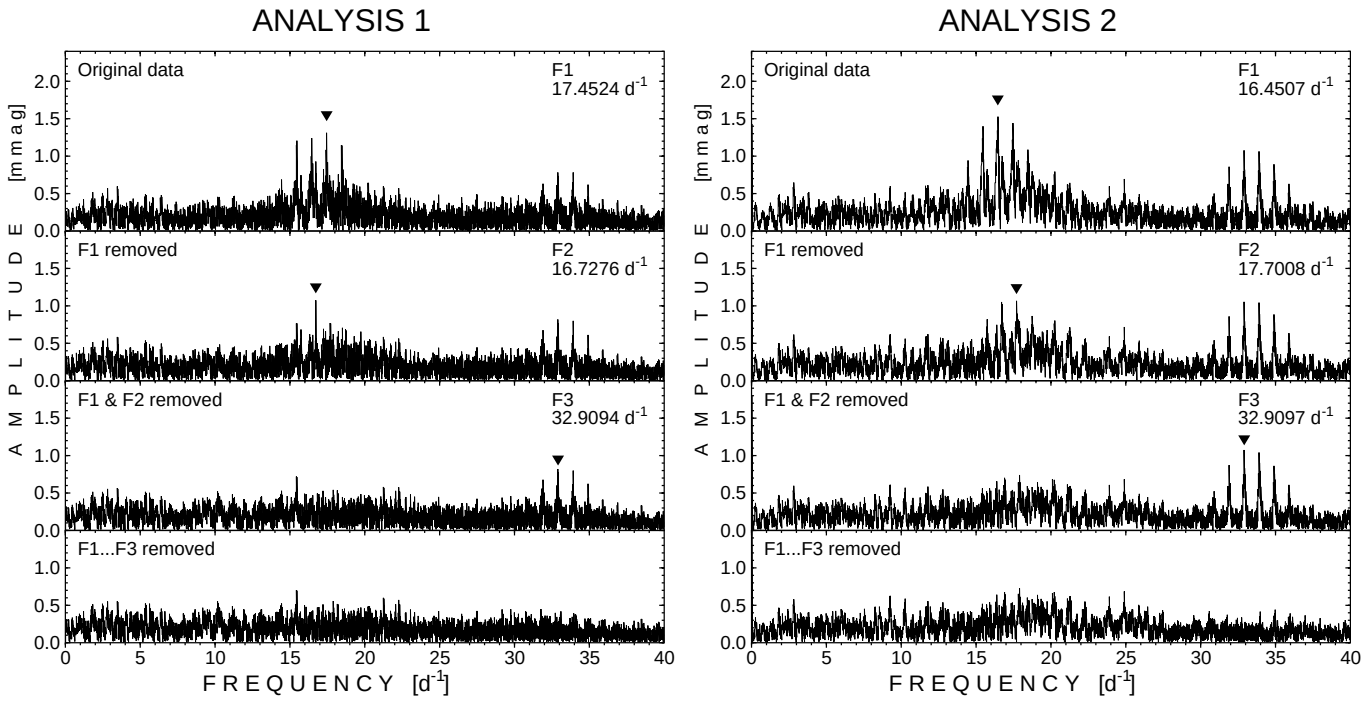

Fig. 8. The same as in Fig. 7, but for the 1998 BV Cnc data.

just below the detection limit, including these modes into the solution would probably change the results for the largest-amplitude modes in an unsignificant way.

By varying weights and by adding a few more modes, we have found rough estimates of the systematic errors on the detected modes. From Table 4 it follows, using the relation $\sigma_{\rm amp} = \sqrt{\pi\sigma^2_{\rm rms}/N}$, that not counting points with low weights and taking $N = 6000$ and $\sigma_{\rm rms} = 0.003$ mmag, we get a noise in the amplitude spectrum of $\sigma_{\rm amp} \sim 0.07$ mmag. With the typical amplitude of the modes in BN Cnc of 2.5 mmag, we expect a $S/N \sim 35$ or an error in the amplitudes of 3%. The S/N in Table 2 are derived from an averaged noise in the residual amplitude spectrum. The values in Table 2 are lower than 35, because of the excess power in the range of the pulsation modes compared to the high frequency part of the spectrum.

Montgomery and O'Donoghue (1999) have derived analytical error formulas for least squares fits. With the same parameters as above and $T = 10$ months we find using their Eqs. (4), (10) and (11): $\sigma(a) = 0.055$ mmag, $\sigma(f) = 0.0005$ μHz and $\sigma(\phi) = 0.022$ rad. The errors of the amplitude, frequency and phase given in Table 2 are only slightly higher than those obtained from the analytical predictions.

7.2. BV Cnc

This star was shown to be a multimode δ Scuti star by Arentoft et al. (1998), where four modes are listed. We have reanalyzed the 1997 data and found somewhat lower amplitudes (see Table 3). One night was rejected and the remaining nights were detrended to remove obvious drift problems. New weights were calculated and bad points rejected. Arentoft et al. (1998) also cleaned the data before deriving their amplitudes.

In 1998 data we find three frequencies (Fig. 8). Owing to the low amplitudes and the shape of our spectral window, an 1 d^{-1} ambiguity in the derived frequencies remains. The frequencies F1 to F3 reported in Table 3 were derived from the combined 1997 and 1998 dataset and then refined by the non-linear least-squares. At the residual periodograms of 1998 data (bottom ones in Fig. 8), F4 can be barely visible. It is, however, obvious that this frequency was present in 1997 data, which can be judged from the bottom panel of Fig. 9 showing the periodogram for 1997 data after removing the first three frequencies. Therefore, we included F4 = 20.246 d^{-1}, which is an 1 d^{-1} alias of A3 derived by Arentoft et al. (1998), as the fourth frequency for BV Cnc.

At the same time, we can clearly see (Fig. 9, Table 3) that not only F4, but amplitudes of all four modes have decreased between 1997 and 1998. In addition, more low-amplitude ($A \leq 0.5$ mmag) modes can be present in the 1998 data because of the excess of power at the residual periodograms (Fig. 8) in the range between 15 and 28 d^{-1}. Their amplitudes are close to the detection limit, so we can only indicate the most promising candidate. This is the peak at frequency of 17.77 d^{-1}.

8. Discussion

The results fall in two categories: the technical or observational aspects and the scientific progress made in this project.

Table 3. Modes detected in BV Cnc. The F4 frequency was derived from the 1997 data only, while frequencies F1 to F3 from the combined 1997 and 1998 data after prewhitening them with F4. Phases and S/N values were derived from the fit to the 1998 data only. The frequencies labeled as $\nu(97)$ were taken from Table 5 of Arentoft et al. (1998). Former ID come also from that paper. Errors are given in parentheses for the last digits.

Our ID	Former ID	Frequency [d^{-1}]	Frequency [μHz]	Amplitudes [mmag] 1997	Amplitudes [mmag] 1998	Phase [rad]	S/N	$\nu(97)$ [μHz]
F1	A1	16.45039(06)	190.3980(07)	2.21(26)	1.45(9)	0.33(06)	7.1	190.47
F2	A2 alias	16.73053(08)	193.6404(09)	1.47(25)	1.08(9)	2.60(08)	5.3	204.83
F3	A4 alias	32.90896(10)	380.8907(12)	1.15(23)	0.79(8)	5.30(11)	4.9	369.10
F4	A3 alias	20.246(4)	234.33(5)	2.18(23)	0.52(8)	4.77(16)	3.7	222.65

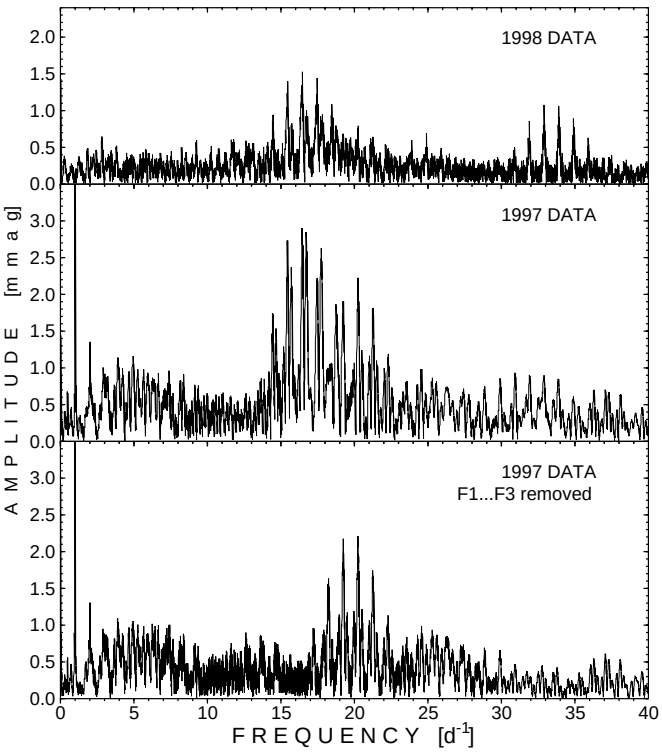

Fig. 9. The evidence for the amplitude change in BV Cnc. Top: LS amplitude spectrum for 1998 data from analysis 2. Middle: the same for 1997 data. Bottom: LS amplitude periodogram of the 1997 data after removing the F1 to F3 frequencies. Note that F4 = 20.246 d^{-1} clearly stands above the noise level.

Table 4. Postfit mean residual standard deviation calculated for all observations from a given site without (RSD_1) and with (RSD_2) weights applied. The last column is the sum of all weights for observations made at a given site presented as a percentage of the summed weights for all observations. The numbers were calculated for the combined 1997 and 1998 dataset for BN Cnc and analysis 1.

Observatory	RSD_1 [mmag]	RSD_2 [mmag]	Contr. %
Tenerife	2.91	2.13	32.0%
Arizona APT	5.61	3.35	17.5%
Konkoly (60 cm)	2.89	2.42	12.3%
Konkoly (100 cm)	4.95	3.49	8.5%
Białków	3.85	3.44	8.2%
Sutherland	5.44	3.03	5.5%
ESO	4.87	3.97	4.0%
La Palma	4.95	3.45	1.5%
UPSO	8.79	—	0.4%
Odessa	12.08	—	0.2%
OHP	—	—	0.0%
1998 data	4.55	2.88	90.1%
1997 data	3.94	3.11	9.9%

8.1. On the differential CCD photometry

Table 4 presents two values for the rms deviation of each datapoint from the final solution for the lightcurve of BN Cnc for each site, as well as the total weight of the dataset as applied in the analysis of the combined time series. The first rms entry is calculated giving equal weight to each point, whereas the second applies the weight used for analysing the lightcurve. Poor measurements enter fully into the first, but are eliminated in the second value. The difference reflects the extent to which the data has been cleaned and weighted.

Looking at Table 4 it is evident that a few sites dominate, partly because of the number of contributed nights, but also due to a higher accuracy for each datapoint.

A few participating sites did not reach the expected accuracy. The distributed observational guidelines obviously were not well enough prepared, that all sites understood the procedures that need to be followed in order to get high quality data. In some cases the instrumentation was not adequate (no autoguider, no overscan of the CCD etc.).

It is also evident that the best CCD photometry outperforms the APT with a photoelectric photometer, which is how it ought to be given that the quantum efficiency of CCDs are higher than for photomultipliers. The factor is, however, small enough that the Arizona site at a different longitude than the CCD sites is very important, not to mention its ease of use. It must be also kept in mind that weather conditions in Arizona were below normal. The value from the third column of Table 4 corresponds well with the values quoted in Sect. 3 obtained for other δ Scuti stars observed with the APT in Arizona.

The sites providing multicolour data show a better S/N in the blue bands. It seems to be an advantage to

observe in the B (or b) band instead of the V (or y) band. The increase in oscillation amplitude going from V to B makes up for the loss of the number of photons.

The window function we obtained (Fig. 7) does not really look like a multisite window function. The alias problem is anyway solved for BN Cnc star due to the presence of data distributed over several months and the low noise level achieved. The high frequency resolution obtained almost guarantees that all detected modes are single.

8.2. Results for the two stars

The noise level in the resulting spectra has been lowered in comparison with earlier observations. It is comparable to the best measurements of other δ Scuti stars. The mode content of the two stars is consequently better defined than before. The presence of some of the modes seen by Arentoft et al. (1998) in the BN Cnc data has not been confirmed. This is important because the parameters derived for BN Cnc depended on these presently undetected modes. This is described in more detail in Paper II.

The amplitudes, frequencies and phases of the six BN Cnc modes are very well determined and provide an excellent baseline for the subsequent analysis of the spectroscopic timeseries presented in Paper II. There is a small bump in the residual noise spectrum in the range 26–30 d^{-1} for this star, but it is difficult to detect any unambiguous modes explaining the presence of this bump.

Evidently the amplitudes of BV Cnc modes have decreased from 1997 to 1998 which is probably best documented by Fig. 9. The difference diminished slightly when a reanalysis was done of the original 1997 data, but the change still remains at a non-ambiguous level. In BV Cnc the presence of several modes close to the detection limit is indicated by a very non-flat residual noise spectrum (see Fig. 8). Opposite to the case of BN Cnc, and due to the low amplitudes we measure, alias problems are quite severe.

It is interesting to note that for BV Cnc the difference between F3 and doubled F1 frequency is very small and amounts to $0.00822 \pm .00016$ d^{-1}. This is almost exactly equal to 3 $yr^{-1} = 0.00821$ d^{-1}. Since it could happen that both F1 and F3 are in error by 1 or 2 yr^{-1}, the possibility that F3 is a harmonic of F1 cannot be rejected. In that case the star would be quite unusual because harmonics are rarely observed for such low-amplitude pulsations. In case it is a pure coincidence, the two modes are very close to the 2:1 resonance which may play an important role in their behaviour.

It should be also pointed out that the two faintest δ Scuti stars in Praesepe, BS Cnc observed by STEPHI (Hernández et al. 1998a) and BV Cnc, display a very similar pattern of excited modes. Both have two or three modes in the range between 15 and 20 d^{-1} and a single mode with frequency over 30 d^{-1}. In other words, BV Cnc matches the pattern of the luminosity dependence of the frequencies excited in Praesepe δ Scuti stars, shown by Belmonte et al. (1997). This means that studying δ Scuti stars in open clusters, especially in Praesepe, could indeed help us to understand the nature of mode selection, constrain cluster parameters and support the mode identification. For this purpose, the work on the other, less extensively observed δ Scuti stars in Praesepe, need to be continued.

9. Conclusions

1. A larger dataset than earlier has been collected for two δ Scuti stars with noise levels of the order of 0.10–0.15 mmag allowing detection of the modes with amplitudes larger than ~0.5 mmag. This is similar to the best campaigns for other δ Scuti stars;
2. The BN Cnc spectrum is well characterized in terms of the existing mode set making the spectral analysis feasible. No significant changes in amplitudes from previous season were found and only one new mode was detected;
3. The BV Cnc spectrum shows a set of low amplitude modes consistent with those previously seen, but with decreased amplitudes;
4. Multisite differential CCD photometry at the best level is a non-trivial job as it involves organizing many sites with good quality equipment and observers familiar with all the procedures.

The data will be made available in the IAU Commission 27 Archives of Unpublished Observations.

Acknowledgements. Part of this work was supported by the German *Deutsche Forschungsgemeinschaft, DFG* project number Ts 17/2–1. This work was also supported in part by grant in Portugal PESO/P/PRO/1196/97″ as well as by the Fund for Scientific Research (FWO) and by the Flemish Ministry for Foreign Policy, European Affairs, Science and Technology. M. Breger and the APT were supported by the Austrian Fonds zur Förderung der wissenschaftlichen Forschung. The IAC80 telescope is operated by the Instituto de Astrofísica de Canarias in the Spanish Observatorio del Teide. The Konkoly team thanks A. Frontó for his collaboration in the observations. The Porto team thanks A. Pedrosa for his collaboration with the observations.

References

Álvarez, M., Hernández, M. M., Michel, E., et al. 1998, A&A, 340, 149

Arentoft, T., Kjeldsen, H., Nuspl, J., et al. 1998, A&A, 338, 909

Baglin, A., Auvergne, M., Catala, C., Michel, E., & the COROT team 2001, Proc. of the SOHO 10/GONG 2000 Workshop Helio- and Asteroseismology at the Dawn of the Millenium, ESA SP-464, 395

Belmonte, J. A., Michel, E., Álvarez, M., et al. 1994, A&A, 283, 121

Belmonte, J. A., Hernández, M. M., Pérez Hernández, F., et al. 1997, in Sounding Solar and Stellar Interiors, ed. J. Provost, & F.-X. Schmider, IAU Symp., 181, 357

Breger, M., & Hiesberger, F. 1999, A&AS, 135, 547
Breger, M., Stich, J., Garrido, R., et al. 1993, A&A, 271, 482
Breger, M., Martin, B., Garrido, R., et al. 1994, A&A, 281, 90
Breger, M., Pamyatnykh, A. A., Pikall, H., & Garrido, R. 1999, A&A, 341, 151
Dall, T. H. 2000, PASPC, 203, 471
Dall, T. H., Frandsen, S., Lehmann, H., et al. 2001, submitted to A&A
Fox Machado, L., Pérez Hernández, F., Suárez, J.-C., & Michel, E. 2001, Proc. of the SOHO 10/GONG 2000 Workshop Helio- and Asteroseismology at the Dawn of the Millenium, ESA SP-464, 427
Frandsen, S. 1992, DSN Newslett., 5, 12
Frandsen, S., Balona, L. A., Viskum, M., et al. 1996, A&A, 308, 132
Handler, G., Pikall, H., O'Donoghue, D., et al. 1997, MNRAS, 286, 303
Hernández, M. M., Michel, E., Belmonte, J. A., et al. 1998a, A&A, 337, 198
Hernández, M. M., Belmonte, J. A., Michel, E., et al. 1998b, in Sounding Solar and Stellar Interiors, IAU Symp., 181 Poster Volume, ed. J. Provost, & F.-X. Schmider, 225
Hernández, M. M., Pérez Hernández, F., Michel, E., et al. 1998c, A&A, 338, 511
Kjeldsen, H., & Frandsen, S. 1992, PASP, 104, 413
Kjeldsen, H., Bedding, T. R., & Christensen-Dalsgaard, J. 2000, PASPC, 203, 73
Matthews, J. M., Kusching, R., & Shkolnik, E. 2001, Proc. of the SOHO 10/GONG 2000 Workshop Helio- and Asteroseismology at the Dawn of the Millenium, ESA SP-464, 385
Michel, E., Hernández, M. M., Houdek, G., et al. 1999, A&A, 352, 153
Montgomery, M. H., & O'Donoghue, D. 1999, Delta Scuti Star Newslett., 13, 28
Pamyatnykh, A. A., Dziembowski, W. A., Handler, G., & Pikall, H. 1998, A&A, 333, 141
Rodríguez, E., López-González, M. J., & López de Coca, P. 2000, A&AS, 144, 469
Sperl, M. 1998, Comm. in Asteroseismology (Vienna), 111, 1
Strassmeier, K. G., Boyd, L. J., Epand, D. H., & Granzer, Th. 1997, PASP, 109, 697
Viskum, M., Kjeldsen, H., Bedding, T. R., et al. 1998, A&A, 335, 549